Article

MULTIBEAM CROSSCHECK ANALYSIS
A Case Study

By Jørgen EEG (DENMARK)
Danish Maritime Safety Administration

Abstract

A new method for analyzing overlapping areas in multibeam surveys is introduced. The method requires that the velocity of sound in the water at the transducer is monitored during the survey. The method applies the principle of least squares to determine the vertical offset and the bias of the swaths caused by insufficient knowledge of the velocity of sound in the water column below the transducer. The precision and robustness of the method is demonstrated on a survey.

Résumé

Une nouvelle méthode d'analyse des zones de chevauchement dans les levés multifaisceaux est ici présentée. Cette méthode impose que la vitesse du son dans l'eau au transducteur soit surveillée pendant l'exécution du levé. Par ailleurs, le principe des moindres carrés est appliqué pour déterminer le décalage vertical et les biais des bandes couvertes que provoque un manque de connaissances de la vitesse du son dans la colonne d'eau sous le transducteur. La précision et la robustesse de la méthode sont démontrées pendant l'exécution du levé.

Resumen

Se presenta un nuevo método para analizar las zonas de solapamiento en los levantamientos multihaz. El método requiere que se controle la velocidad del sonido en el agua del transductor durante el levantamiento. Este método aplica el principio de los mínimos cuadrados para determinar el desfase vertical y las distorsiones de las zonas exploradas causadas por un conocimiento insuficiente de la velocidad del sonido en la columna de agua situada bajo el transductor. La precisión y la resistencia del método se demuestran durante un levantamiento.

Introduction

S-44 Annex A – Guidelines for Quality Control (S-44 2008) recommends that depth data integrity in multibeam surveys is controlled by check lines or overlapping swaths using a '*quality control procedure* (which) *should include statistical analysis of differences and the consideration of common errors to provide an indication of compliance of the survey with the standards given in* (Minimum Standards for Hydrographic Surveys)'. The present case study presents a modus operandi for a multibeam crosscheck analysis which has an impact on the planning of multibeam surveys in which the velocity of sound in the water at the transducer is measured continuously during the survey. The Cross-Section method, which is treated in detail below, takes advantage of the fact that detailed knowledge of the sound speed profile is not needed in order to correct soundings, by employing the principle of least squares to estimate corrections to measured profiles. This makes it possible to improve casts taken by traditional methods or, alternatively, to separate long periodic errors i.e. biases from the noise when the a posteriori error budget is put together.

***Figure 1*.**
Distribution of cells in DTM of survey track (red) and check line (white).

The fact that the Minimum Standards for Hydrographic Surveys (S-44 2008) relate the soundings to the true position of the sea bed, forces the quality control of a multibeam survey to aim at verifying whether or not the different sensors entering into the multibeam equation adhere to the specs stated by the manufacturer. In case they do, the reasoning is that the a priori error budget of the survey then presents a true picture of the distribution of the soundings relative to the sea bed. It follows that approaches to disclose artefacts in the survey are at a premium. The author's method of choice is the following. For a given cell size, which, as a rule-of-thumb, may be as large as 10% of the depth, construct a DTM of the soundings which covers the intersection between the survey lines. Following a long tradition in hydrography, the smallest depth inside each cell determines the height of the cell, but for our purpose we shall be more interested in to which of the two tracks the sounding and therefore the cell belongs. A census of the number of cells belonging to the two tracks may be compared to the expected number using statistics, see (Eeg 2004). When the issue is disclosure of artefacts, ***Figure 1*** illustrates that this method of analysis cannot stand alone, but must be supplemented by an evaluation of the pattern of the blending of the cells belonging to the two tracks. ***Figure 2*** illustrates the power of this method. The eye catches the surplus of red cells to the right and of white cells at the bottom of the intersection which, together with the added information that the tracks were surveyed towards North and East respectively, causes the analyst to suspect a minor roll calibration error. This was confirmed by using the method in (Eeg 2008), changing the angle by 0.03°.

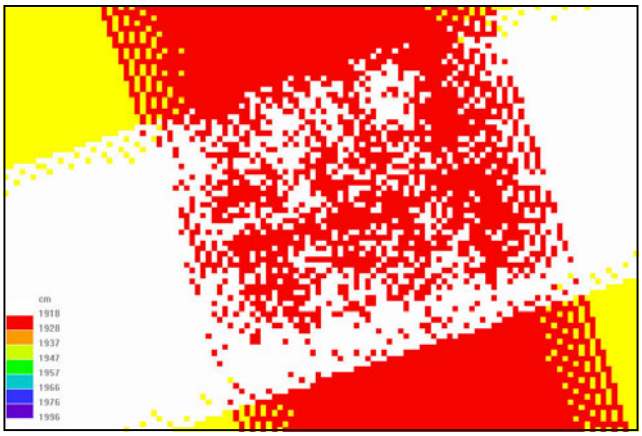

Figure 2
Small artefact from incorrect roll calibration of multibeam echo sounder

By the way, the two tracks depicted in ***Figure 1*** were randomly chosen from a RTK survey. For experimental purposes the ray tracing of the soundings was based only on the measured velocity of sound (s/v) at the transducer placed at the bottom of the vessel. The Cross-Section method yielded estimates of correction to the s/v profile and to the *vertical* displacement between the two tracks of -8.0m/s, -6.5m/s and 0.5cm respectively. Figure 2 depicts a DTM of the two tracks after the ray tracing was corrected by adding the estimated s/v's to the measured values in the profiles, starting just below the transducer.

The Cross-Section method

Following the layout of the ship lanes, most of the hydrographic surveying in Danish waters is conducted along parallel lines.

While this method is optimal only when the depth along the survey line is constant, the fringe benefit of varying depths is that the overlapping swaths between neighbouring lines may be used to assert the quality of the survey. Considering that the sea bed in general is smooth, the check up ought to be a piece of cake. It is not, however, because the s/v profile below the survey vessel as a rule is quickly changing from place to place. In order to establish some measure of control the Danish survey vessels have since 1999 measured the s/v at the transducer at all times during survey. It holds true that, if the s/v at the transducer is known, the vertical movement Δz of the soundings in a swath for small relative changes in the s/v to a linear approximation is governed by the formula

$$\Delta z \simeq d \cdot \overline{\rho} \cdot (1 - \tan^2 \theta) \qquad (1.1)$$

d being the (observed) depth difference between the sounding and the transducer, $\overline{\rho}$ the average relative change in the s/v in the water column and the launch angle θ is measured relative to the Nadir (Eeg 1999). The relation is (2.9) derived in the appendix. (Eisler 2000) demonstrates that the ray-path stability quickly deteriorates for launch angles beyond 60°, so as a rule of thumb we shall limit the Cross-Section method to data sampled within this angular sector and be wary of values of $\overline{\rho}$ exceeding 2%. In the shallow Danish waters these precautions will ensure the validity of (1.1), even for small perturbations of the s/v at the transducer, see (Eisler 2000).

In a region where swaths from two survey lines overlap, we may consider the average relative errors in the s/v profiles $\overline{\rho_1}$ and $\overline{\rho_2}$ together with the vertical displacement $\delta_{1,2}$ between the two lines, to be constant, but unknown, if the region is small enough. In order to fix the ideas, the reader may think of $\delta_{1,2}$ as representing errors in correction for tide, vessel settlement etc., but any slowly varying error in the direction of the plumb line, as for example displacements caused by unfavourable satellite constellations in RTK, will do. Suppose now that we construct two DTMs, one for the survey line and the other for the check line, both covering the intersection, in such a way that each cell i in the two DTMs covers the same area of the sea bed.

Suppose furthermore that the cell size is so small, that we can consider the (unknown) depth of the sea floor in a cell, D_i, to be constant. Then, for each of the two tracks, we find

$$d_{j,i} + d_{j,i}(1 - \tan^2 \theta_{j,i})\overline{\rho_j} + \Delta_{j,i} = D_i \qquad j = 1,2 \qquad (1.2)$$

where the (unknown) corrections $\Delta_{j,i}$ satisfy the relation

$$\Delta_{1,i} - \Delta_{2,i} = \delta_{1,2} + \varepsilon_i$$

The difference between the two equations in (1.2) yields at each cell in the region an observation equation

$$d_{1,i} \cdot (1 - \tan^2 \theta_{1,i}) \cdot \overline{\rho_1} - d_{2,i} \cdot (1 - \tan^2 \theta_{2,i}) \cdot \overline{\rho_2} + \delta_{1,2} = d_{2,i} - d_{1,i} + \varepsilon_i \qquad (1.3)$$

and it makes sense to fit the two surfaces together by seeking values of the unknowns, $\widehat{\rho_1}$, $\widehat{\rho_2}$ and $\widehat{\delta_{1,2}}$, which minimize the sum of the squared errors $\sum \varepsilon_i^2$.

Having ended up in a classical least squares adjustment, the inverse to the normal equation matrix, i.e. the variance-covariance matrix, is the key to the precision of the unknowns and indeed, being small-dimensional it can be readily evaluated in each particular case whenever data is available. In order to be able to take full advantage of the method, however, it is necessary to investigate how the precision of the unknowns depends on the angle between the survey line and the check line.

Design considerations in crosscheck analysis

Figure 2 may have seduced the reader into believing that the Cross-Section method is very precise and indeed its power is demonstrated on a survey below. However, an inspection of equation (1.3) reveals, other things being equal, that the solution breaks down if the check line is placed exactly on top and parallel to the survey line. In this case the coefficient to the first two unknowns in each of the observation equations become equal with opposite signs, i.e. the two unknowns can only be determined up to a common constant. Geometrically this means that the swaths in the two lines can be bended so that they coincide, leaving the correct common curvature undetermined. When the check line is placed parallel to the survey line so that the overlapping area only consists of the outermost set of beams, the situation is quite contrary. In order to see that, place a co-ordinate system with origin at the transducer, z-axis positive down along the plumb line and x-axis orthogonal to the z-axis so that the swath is spanned by the x-z plane.

In this co-ordinate system any change in the ray trace of the soundings, caused by a perturbation of a s/v profile which only depends on z, is an even function of *x*. We can change parameters in (1.1) by setting

$$x = d \cdot \tan\theta$$

yielding

$$\Delta z = (\overline{\rho}/d)(d^2 - x^2) \qquad (1.4)$$

Suppose the centre of the overlap between the two parallel tracks has abscissa *a*, then in the parallel track its abscissae is *–a* and we can determine the slopes of the two tracks such that they coincide at the intersection. In fact, for a given value of $\overline{\rho}_1$ we can determine $\overline{\rho}_2$ so that the equality

$$\frac{2a\overline{\rho}_1}{d_1} = -\frac{2a\overline{\rho}_2}{d_2}$$

holds, and then the observations in the overlapping zone only differ by a common vertical displacement. This displacement, however, depends on the choice of $\overline{\rho}_1$ In general, then, we should either have a relatively large overlap or reliable estimates of the s/v errors before we estimate a difference in level between neighbouring survey lines.

The Cross-Section method yields reliable estimates of the s/v errors if the control line is surveyed at right angles to the survey lines. The reason is that, at the area of intersection, all soundings in any given swath belonging to the control line are placed within the same small angular sector seen from the transducer when the survey line was measured, so that any s/v error in the control line is measured against the correct form of the sea bed, albeit shifted vertically by the s/v error in the survey line. For reasons of symmetry this argument holds true for the swaths of the survey line with respect to the control line too.

In the above discussion of the method it is understood that an adequate cell size is chosen. If the cell size is too large, the two DTMs lack the flexibility to react adequately to subtle changes in the curvature of the sea bed, resulting in poor estimates of the $\overline{\rho}$'s followed by a poor estimate of the standard deviation between the two data sets. On the other extreme, the cell size may become so small, that information is lost by reducing the set of cells with contributions from both data sets. The investigation below indicates that there is some robustness in the method as regards the choice of cell size and ways to safeguard against these extremes.

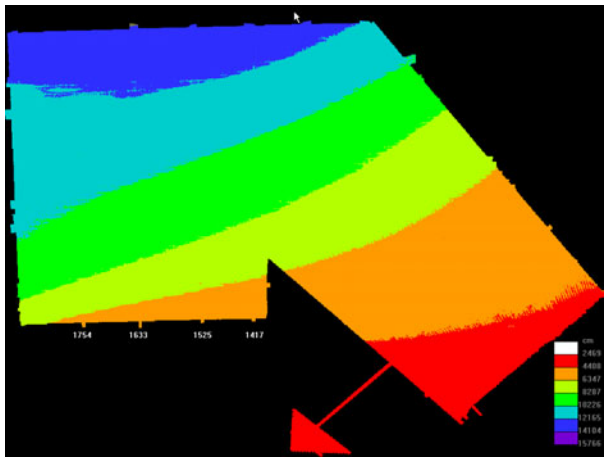

Figure 3
DTM of 00309, cell size 6m. Reson SeaBat 7125 200kHz

Survey 00309

00309 is the third compact area surveyed in 2009 by HDMS Jens Sørensen. The survey was RTK, the echo sounder a Reson SeaBat 7125 200 kHz with a SVP-70 to monitor the s/v at the transducer. Most of the s/v below the transducer was sampled as discrete profiles by an ASV5002, the ScanFish only being functional at the end of the survey. Figure 3 depicts the depth variation in the area.

Figure 4 depicts the lay out of the survey lines and check lines. Five parallel check lines were selected because of their lengths. Four of the check lines were surveyed at 28 August while the fifth, painted red in Figure 4, was surveyed at 1 September in bad weather, the vessel going into harbour after completing the line. The survey time for each of the four lines is depicted below each line in Figures 3 and 4. The common s/v profile used for the four check lines was sampled immediately before they were surveyed at 28 August 14:04. Below this profile is referred to as profile 14:04. Its position is indicated by the mouse cursor in form of an arrow near top of the image in both figures.

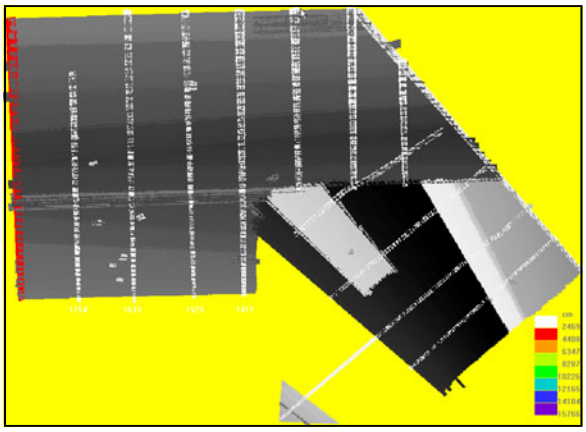

Figure 4
Layout of check lines in 00309

The Cross-Section method was employed on the intersections of 44 parallel survey lines with the five check lines. Throughout the cell size for the observations equations was 6m, using an average whenever more than one contribution fell into a cell. For reasons of presentation, the resulting estimates of the average relative error in the s/v profile were multiplied by 1465 m/s in order to convert them into quantities which could be related to the entries in the s/v profile. The normal variation of the s/v in Danish waters is between 1430m/s and 1500m/s, so the error in multiplying by 1465 is less than 3%.

Figure 5 depicts the variation of the estimates of the average s/v error in profile 14:04 for each of the four check lines surveyed at 28 August. The axis of abscissa represents survey lines, numbered from top to bottom and the units of the ordinate axis are m/s. The fact that the same s/v profile has been used for each of the four check lines makes a direct comparison between the four graphs meaningful. Given that the s/v profile was measured at the deep end of the area, one would expect all the graphs to start at zero. They do not, however, because the signature (Eeg 2008) of the Reson SeaBat 7125 changes the across track shape of the sea bed, depending on the hydrophone and on the version of the maintenance release. The odd component of this change is compensated by the calibration for roll, whereas the even part fools the surveyor into believing that his s/v profiler needs to be calibrated. Apart from this, at least two facts are worth attention in Figure 5. The first is the high correlation of each graph with the variation of the depth at the corresponding check line, as seen from Figure 3. The second is the size of the variation from survey line to survey line as the crossings by the check lines move from top to bottom.

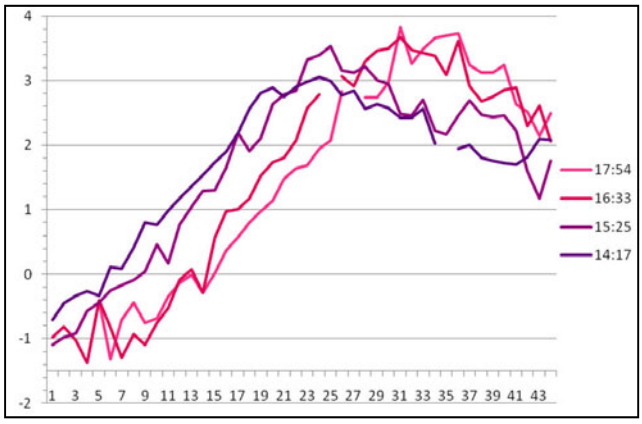

Figure 5
Estimates of the average error in profile 14:04 for four check lines 28 August 2009. Cell size 6m

The average error in the s/v profile for the fifth check line is not depicted. Keeping within ±0.5m/s of an average value of 1.5m/s, the lack of variation is probably caused by turbulence in the water due to the weather conditions.

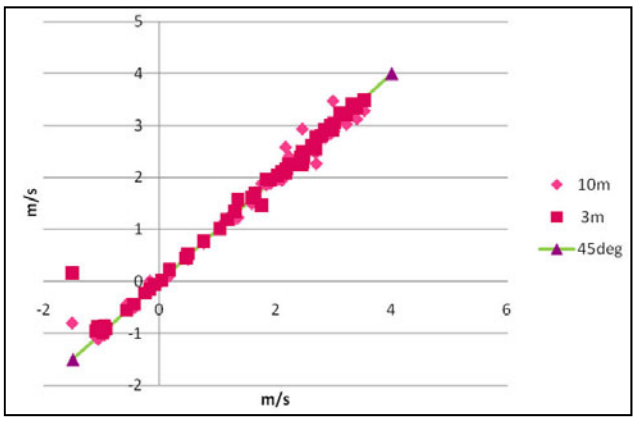

Figure 6
Plots of estimates from 6m cell size against 3m and 10m for 44 crosses of check line 15:25

In order to check up on the robustness of the estimates with respect to the chosen cell size, the Cross-Section method was recalculated for the check line surveyed 28 August at 15:25 using cell sizes of 3m and 10m. ***Figure 6*** depicts plots of the estimates of $\overline{\rho}$ from 44 homologous crossings in cell sizes 6m against 3m (red) and 6m against 10m (blue). A green line depicting positions of no influence from change in cell size serves to evaluate the variation. It appears from the figure, that the estimates are robust with respect to these variations in the cell size, the 10m cell size displaying a slightly larger variation than the 3m.

A simulation model

Above it was claimed that if the s/v at the transducer is known, then (1.1) is a valid approximation to the vertical change of a swath as a function of change in the s/v profile in the shallow Danish waters, provided that the angular sector in the swath is confined to the interval [60°, 60°] and the average relative change in the s/v profile is below 2%. As a rule of thumb, at 100m below the transducer a 1m/s average change in a profile changes the depth by 7cm, while the change at 60° is twice this amount with opposite sign. For a given s/v profile, however, it is of interest to verify that these claims hold true. The profile is extended by interpolating the discrete measurements linearly so that the ray-path segments become circular arcs. Suppose now that the profile at hand exactly represents the variation of the s/v, then we can calculate the travel times for a set of launch angles in the interval [0°,60°] from the top of the profile to an arbitrary, but fixed, depth *D*.

In order to emulate survey conditions, a s/v profile, which is close to the profile and coincides with it at transducer depth, is chosen to simulate a measured survey profile. At each launch angle θ_i , then, the survey profile and travel time is used to find the depth d_i ,i.e. in the spirit of equation (1.2) we have a set of observations equations

$$d_i(1-\tan^2\theta_i)\rho = D - d_i + \varepsilon_i$$

from which we find the estimate $\hat{\rho}$ of ρ which minimizes the sum of squared errors $\sum\varepsilon_i^2$ to be

$$\hat{\rho} = \sum d_i(1-\tan^2\theta_i)(D-d_i)\Big/\sum d_i^2(1-\tan^2\theta_i)^2$$

The estimate results in an adjustment of the simulated survey profile, except at transducer depth where the value is fixed.

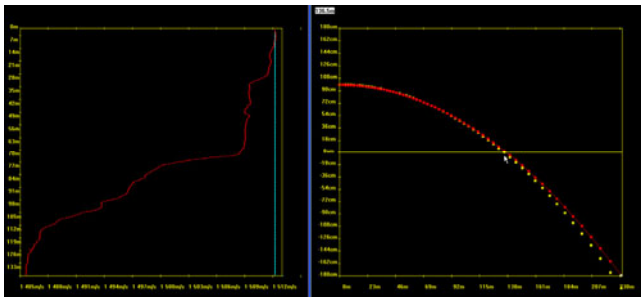

Figure 7
Left profile 14:04 (red) and the default survey profile (cyan) Right the perturbation of the sea bed (red) and the least squares approximation (yellow)

The case in point is profile 14:04 for which the Cross-Section method yielded corrections between -1.5m/s and 4m/s in Figure 4. In order to push the simulation model to its logical conclusion we shall as survey profile choose the default survey profile, which at any depth equals the value measured at transducer depth. It is tacitly understood, that if the adjusted default profile at some depth *D* approximated profile 14:04 well, then the adjustment at that depth read from Figure 4 applied to profile 14:04 is OK too. **Figure 7** left depicts the two profiles. ***Figure 7*** right depicts (in red) $d_i - D$ from the right hand side of the observations equations together with the corresponding least squares estimates (in yellow), for the set of integer angles below 60° with *D*=136.5m. ***Figure 8*** right depicts the least squares residuals $\hat{\varepsilon}_i$, i.e. the depth differences at 136.5m caused by exchanging profile 14:04 with the adjusted default profile. This result only relates to the depth 136.5m, of course. ***Figure 8*** left illustrates the consequence of exchanging the two profiles 10m above the sea bed at 126.5m.

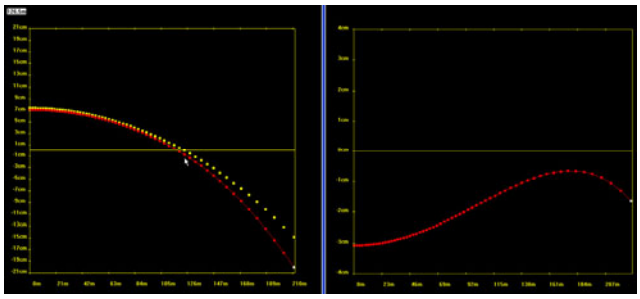

Figure 8
Change in depth caused by exchanging profile 14:04 with the adjusted default profile at 126.5m (left) and 136.5m (right)

Table 1 quantifies the differences between profile 14:04 and the adjusted default profile by depicting estimated standard deviations of the horizontal and vertical displacements based on ray-tracing for the set of integer launch angles between 0° and 60°, together with the vertical difference between the two profiles at launch angles 0°, 45° and 60°. The table depicts also the variation of this set of values for changes of ±0.2m/s at transducer depth for the default profile.

Table 1
The simulation model applied to profile 14:04 and the adjusted default profile at depth 136.5m

Online	Vertical	Horiz.	Error at	Error at 45°	Error at 60°	$\hat{\sigma}$
s/v	stddev.	stddev.	0°			
+0.0m/s	0.024m	0.035m	0.03m	0.01m	0.02m	-10.5m/s
-0.2m/s	0.038m	0.036m	0.04m	0.03m	0.05m	-10.4m/s
+0.2m/s	0.017m	0.035m	0.02m	-0.01m	-0.02m	-10.6m/s

For reference, for the SVP-70 which was used to measure the s/v at the transducer depth during the survey, the factory specifies a standard deviation of 0.025m/s.

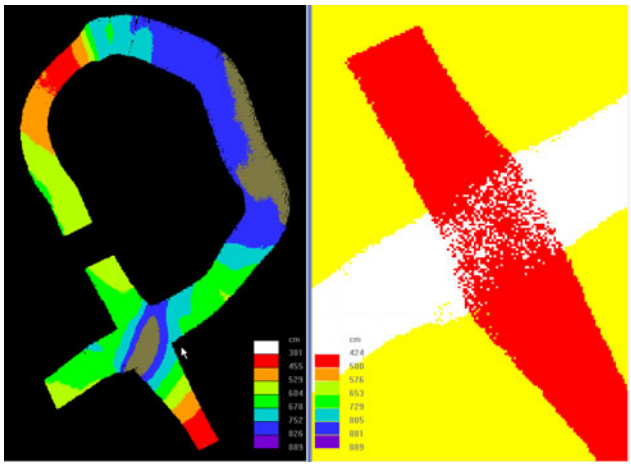

Figure 9 *Loop survey. Cell size 60cm. Reson SeaBat 8101*

The loop

Figure 6 demonstrated the robustness of the estimates with respect to cell sizes for survey 00309. The sea bed of this survey is flat relative to the sizes of the crossings of the survey lines with the check lines, a characteristic it shares with most of the sea bed in Danish waters. The question arises if the Cross-Section method requires the sea bed to be flat in order to yield usable estimates. ***Figure 9*** depicts a DTM with cell size 60cm of a loop surveyed by HDMS O-2 using a SeaBat 8101 with a SVP-C mounted at transducer depth. In order to stress the method, the crossing was positioned on top of a 1.5m deep depression in the sea bed on 6m of water. Once more the survey was RTK and the blending of the cells in the close up of the intersection to the right in the figure testifies to the integrity of the sensors.

Table 2
Parameter estimates for the loop for various cell sizes.

Cell size	$\widehat{\rho_1}$	$\widehat{\rho_2}$	$\widehat{\delta_{1,2}}$	$\widehat{\sigma_{1,2}}$
25 cm	0.18 m/s	0.11 m/s	1.6 cm	2.8 cm
30 cm	0.23 m/s	0.06 m/s	1.7 cm	2.5 cm
40 cm	0.48 m/s	0.20 m/s	1.7 cm	2.2 cm
50 cm	0.57 m/s	0.15 m/s	1.8 cm	1.9 cm
60 cm	0.73 m/s	0.33 m/s	1.7 cm	1.7 cm
70 cm	0.87 m/s	0.57 m/s	1.7 cm	1.5 cm
80 cm	1.05 m/s	0.82 m/s	1.7 cm	1.6 cm
100 cm	1.40 m/s	0.88 m/s	1.8 cm	1.6 cm
150 cm	2.83 m/s	1.94 m/s	1.8 cm	2.6 cm
200 cm	4.67 m/s	3.20 m/s	2.0 cm	3.5 cm
250 cm	6.99 m/s	5.19 m/s	2.1 cm	4.3 cm

Table 2 depicts estimates for the loop using cell sizes ranging from 25 cm to 2.5m. The last column in the table contains the square root of the a posteriori variance factor, i.e. estimates of the standard deviation $\widehat{\sigma_{1,2}}$ between the two DTMs after the corrections have been applied to data.

Now, by construction the second and third column should be equal for a fixed cell size, because the crossing lines were near simultaneous. Considering that a 1m/s deviation at 7m from (1.1) corresponds to 1cm at 60° I think the reader will agree that the variation in Table 2 is acceptable.

The variation with respect to the cell sizes, however, is another matter, because the estimates rapidly become meaningless concurrently with the DTMs lacking ability to represent the sea floor. In case that there are no artefacts in data, and indeed from the blending of the cells in Figure 9 everything looks OK, it makes sense to choose the cell size 70cm which minimizes the variance between the two DTMs, although any choice between 50 cm and 1m probably will be of use.

Discussion

In hydrographic surveying, s/v in the water below the vessel is measured in profiles and a model for the variation of the s/v is adopted, in which it only depends on the depth. Any change in the s/v profile relative to the measured one will then, at a fixed depth *D*, lead to a perturbation *f(.)* for which *f(x)=f(-x)* in the co-ordinate system introduced above. In mathematical parlance *f(.)* is an even function and may be represented to any prescribed degree of accuracy by some polynomial in even powers of *x*. Considering that experience shows, that multibeam measurements react to errors in the s/v profile by bending the swath gently, it is not surprising that this bending can be approximated very well by a polynomial of degree 2. The fact worth noticing, however, is that when the s/v at the transducer is known the approximating polynomial belongs to a special class (1.4) which leaves the depth at ±45° unchanged (1.1). The reason that it is so does not follow directly from (2.7), because tools like Hölder's inequality by their very nature are pessimistic and indeed, even in the shallow Danish waters one cannot expect the approximation to be good in the interval [-75°,75°] which is the standard range of many multibeam systems. Restricted to the interval [-60°, 60°] in shallow water, the matter is different. For example, the simulation model applied to 5793 s/v profiles sampled in waters deeper than 10m yields 207 cases where the change at 45° exceeds 1cm and 78 cases where it exceeds 2cm. Profile 14:04 is one such case and it is worth noticing, that even though the change at 45° is at the tail of the distribution, the residual from the approximation, depicted in Figure 6 right, is a polynomial of degree 4, just as one would expect.

Acknowledgement

I gratefully acknowledge the many fruitful suggestions to the manuscript from Thomas Eisler.

References

IHO Standards for Hydrographic Surveys (S-44) 5th Edition, Annex A – Guidelines for Quality Control, February 2008.

Eeg, J. (2004) Verification of the Z-Component in the RTK Survey of Drogden Channel. *International Hydrographic Review*, Vol. 5 No. 2, 16-25.

Eeg, J. (2008) On the Roll Calibration of a Multibeam Echo Sounder. Unpublished.

Eeg, J. (1999) Towards Adequate Multibeam Echosounders for Hydrography. *International Hydrgraphic Review,* Vol. LXXVI No. 1, 33-48.

Eisler, Thomas J. (2000) Ray-path Stability in Coastal Waters. *International Hydrographic Review*, Vol.1 no.2, 30-40.

Appendix

Let the surface of the transducer coincide with the origin of a co-ordinate system, where the z-axis points towards the Nadir. The travel time T from the moment the ping leaves the transducer in the direction θ_0 with the z-axis until it reaches the depth d is given by the integral

$$T = \int_0^d \frac{dz}{C\cos\theta} \qquad (2.1)$$

where the velocity of sound in water,C, is supposed only to depend on the depth z and the angle θ is found from Fermat's principle as

$$\frac{\sin\theta_z}{C_z} = p \quad , \qquad z \in [0, d] \qquad (2.2)$$

p being Snell's constant, the value of which for any given launch angle, θ_0 , we shall suppose is found from s/v measurements at the transducer. Suppose now, that the value of the velocity of sound in water is changed according to

$$C_z \mapsto C_z + \Delta C_z = C_z(1+\rho_z) \quad , \quad z \in]0, d]$$

while it is kept fixed at the transducer. Then, from (2.2), for the same launch angle θ_0 , the angle is changed in the water below the transducer according to

$$\frac{\sin(\theta_z + \Delta\theta_z)}{C_z(1+\rho_z)} = \frac{\sin(\theta_z)(1+\rho_z)}{C_z(1+\rho_z)} = p, \qquad z \in]0, d] \qquad (2.3)$$

By (2.1) the difference in time ΔT between the two paths becomes

$$\Delta T = \int_0^d \frac{dz}{C\cos\theta} - \int_0^d \frac{dz}{C(1+\rho)\cos(\theta+\Delta\theta)}$$

or,

$$\Delta T = \int_0^d \left[1 - \frac{1}{(1+\rho)\sqrt{\frac{1-\sin^2(\theta+\Delta\theta)}{\cos^2\theta}}}\right]\frac{dz}{C\cos\theta}$$

Using (2.3) we find

$$\Delta T = \int_0^d \left[1 - \frac{1}{(1+\rho)\sqrt{1-\rho(2+\rho)\tan^2\theta}}\right]\frac{dz}{C\cos\theta}$$

Expanding the square root in the absolute convergent binomial series

$$\frac{1}{\sqrt{1-\rho(2+\rho)\tan^2\theta}} = 1 + \frac{\rho(2+\rho)\tan^2\theta}{2} + R(\rho(2+\rho)\tan^2\theta)$$

with remainder *R()* we find

$$\begin{aligned}\Delta T = &\int_0^d \frac{1-\tan^2\theta}{C\cos\theta}\cdot\frac{\rho dz}{1+\rho} \\ &- \int_0^d \frac{R(\rho(2+\rho)\tan^2\theta) + \tfrac{1}{2}\rho^2\tan^2\theta}{1+\rho}\cdot\frac{dz}{C\cos\theta}\end{aligned} \qquad (2.4)$$

For the remainder we have

$$R(y) = \frac{\frac{1}{2}(\frac{1}{2}+1)y^2}{2!} + \ldots + \frac{\frac{1}{2}(\frac{1}{2}+1)(\frac{1}{2}+2)\ldots(\frac{1}{2}+n)y^{n+1}}{(n+1)!} + \ldots$$

Or

$$R(y) = \frac{3y^2}{8}\left[1 + \frac{5y}{6} + \frac{5\cdot 7\,y^2}{6\cdot 8} + \ldots + \frac{5\cdot 7\cdots(2n+1)y^{n+1}}{6\cdot 8\cdots(2n+2)} + \ldots\right]$$

So that

$$R(y) \le \frac{3y^2}{8(1-y)} \qquad (2.5)$$

Let

$$\bar{\rho} = \frac{1}{d}\int_0^d \frac{\rho dz}{1+\rho} \quad and \quad \bar{\delta} = \frac{1}{d}\int_0^d \frac{1-\tan^2\theta}{C\cos\theta}dz \qquad (2.6)$$

Then we can write the first integral in (2.4) as

$$\int_0^d \frac{1-\tan^2\theta}{C\cos\theta}\cdot\frac{\rho dz}{1+\rho} = \int_0^d \frac{1-\tan^2\theta}{C\cos\theta}\rho dz + \int_0^d \left[\frac{1-\tan^2\theta}{C\cos\theta} - \bar{\delta}\right]\left[\frac{\rho}{1+\rho} - \bar{\rho}\right]dz$$

and (2.4) becomes

$$\Delta T - \int_0^d \frac{1-\tan^2\theta}{C\cos\theta}\rho dz = \int_0^d \left[\frac{1-\tan^2\theta}{C\cos\theta} - \bar{\delta}\right]\cdot\left[\frac{\rho}{1+\rho} - \bar{\rho}\right]dz - \int_0^d \frac{R(\rho(2+\rho)\tan^2\theta) + \tfrac{1}{2}\rho^2\tan^2\theta}{1+\rho}\cdot\frac{dz}{C\cos\theta}$$

Where we can use Hölder's inequality on the integrals on the right side of the equality sign to get

$$\left|\Delta T - \int_0^d \frac{1+\tan^2\theta}{C\cos\theta}\rho dz\right| \le \left\|\frac{1-\tan^2\theta}{C\cos\theta} - \bar{\delta}\right\|_2 \left\|\frac{\rho}{1+\rho} - \bar{\rho}\right\|_2 + \left\|\frac{R(\rho(2+\rho)\tan^2\theta) + \tfrac{1}{2}\rho^2\tan^2\theta}{1+\rho}\right\|_\infty \left\|\frac{1}{C\cos\theta}\right\|_1$$

Or, using (2.1) and (2.5)

(2.7)

$$\left|\Delta T - \int_0^d \frac{1-\tan^2\theta}{C\cos\theta}\rho dz\right| \le \left\|\frac{1-\tan^2\theta}{C\cos\theta} - \bar{\delta}\right\|_2 \left\|\frac{\rho}{1+\rho} - \bar{\rho}\right\|_2 + \sup\left[\frac{\frac{3(\rho(2+\rho)\tan^2\theta)^2}{8(1-\rho(2+\rho)\tan^2\theta)} + \tfrac{1}{2}\rho^2\tan^2\theta}{1+\rho}\right]T$$

Now, for a given depth d and s/v profile we can for any $\varepsilon > 0$ find values $\rho_0 > 0$ and $\theta_0 > 0$ so that

$$\left|\Delta T - \int_0^d \frac{1-\tan^2\theta}{C\cos\theta}\rho dz\right| < \varepsilon \quad \forall|\rho| < \rho_0 \wedge \forall|\theta| < \theta_0 \qquad (2.8)$$

In order to be of interest for multibeam surveying, however, it is necessary that (2.8) for sufficiently small ε holds for $\theta_0 .> \pi/4$, so that the minimum of the integral implies that ΔT, regarded as a function of θ, attains a minimum at $\theta \simeq \pm\pi/4$ too. In the Danish Maritime Safety Administration it is natural to consider (2.8) for values of θ inside $[-\pi/3,\pi/3]$ because observations in a swath outside this angular sector are flagged out automatically during post-processing. For launch angles inside this sector, inspection of more than 13000 s/v profiles sampled during the period 2000 to 2009 shows, that (2.1) is well defined at the depth of the bottom of the profile. Moreover, measuring the variation of the s/v in the profile relative to the s/v at the transducer,

$$C_z = C_0(1 + \mathrm{P})$$

$|\mathrm{P}|$ was found to be less than 1% for five out of six profiles, whereas it was larger than 2% for 2% of the profiles. In terms of angular variation of the ping through the water column (2.3) yields, that for a launch angle of 60° the ray path varies between ±1° and ±2° respectively. These deviations decrease with decreasing launch angles, being diminished by almost one half at a launch angle of 45°, so we can write

$$\Delta T \simeq \int_0^d \frac{1-\tan^2\theta}{C\cos\theta}\rho dz \simeq \frac{d(1-\tan^2\theta_0)\bar{\rho}}{C_d\cos\theta_d} \qquad (2.9)$$

Or, using the differential form of (2.1)

$$\Delta z \simeq d(1-\tan^2\theta_0)\bar{\rho}$$

Biography of the author

Jørgen Eeg is head of validation of hydrographic data at the Danish Maritime Safety Administration. He gradated as a geodesist from the University of Copenhagen in 1972 and worked with approximation of the potential field of the earth by collocation, integrated geodesy and continuous modelling of plane networks until 1987. At that time the emerging graphic capabilities of workstations and the need to automate work with large data sets led him, following a brief spell of digital picture processing and digital cartography, into the field of hydrography, where he has worked since 1990.
e-mail: eeg@frv.dk